

Supplementary Materials for

mDia1/3-dependent actin polymerization spatiotemporally controls LAT phosphorylation by Zap70 at the immune synapse

D. Thumkeo*, Y. Katsura, Y. Nishimura, P. Kanchanawong, K. Tohyama, T. Ishizaki, S. Kitajima, C. Takahashi, T. Hirata, N. Watanabe, M. F. Krummel, S. Narumiya*

*Corresponding author. Email: d.thumkeo@mfour.med.kyoto-u.ac.jp (D.T.); snaru@mfour.med.kyoto-u.ac.jp (S.N.)

Published 1 January 2020, *Sci. Adv.* 6, eaay2432 (2020)
DOI: 10.1126/sciadv.aay2432

The PDF file includes:

Supplementary Materials and Methods

Fig. S1. Effects of formin inhibition after initial TCR microcluster formation in naïve CD8 OT-I T cells stimulated on SLBs.

Fig. S2. TCR signaling in naïve CD8 T cells from mDia1 KO or mDia3 KO mice.

Fig. S3. Dynamic localization of EGFP-mDia3 in the IS.

Fig. S4. IS spreading and TCR microcluster centralization are impaired in mDia1/3 cDKO naïve CD8 OT-I T cells.

Fig. S5. T cell lymphopenia results from impaired positive selection in mDia1/3 DKO mice.

Fig. S6. T cell development in mDia1 KO mice and mDia3 KO mice.

Fig. S7. Impaired T cell development phenotypes in mDia1/3 DKO are cell intrinsic.

Fig. S8. Conditional deletion of mDia1 and mDia3 in the T cell lineage.

Fig. S9. mDia1/3 deficiency impaired thymocyte-positive selection in OT-I and OT-II transgenic mice.

Fig. S10. Impaired TCR microcluster centralization and peripheral F-actin ring formation following loss of mDia1/3 in OT-I thymocytes.

Other Supplementary Material for this manuscript includes the following:

(available at advances.sciencemag.org/cgi/content/full/6/1/eaay2432/DC1)

Movie S1 (.mov format). TIRF live imaging of TCR microcluster dynamics in a control naïve CD8 OT-I T cell stimulated on a SLB (2 s per frame; 60 frames).

Movie S2 (.mov format). TIRF live imaging of TCR microcluster dynamics in a 10 μ M SMIFH2-treated naïve CD8 OT-I T cell stimulated on an SLB (2 s per frame; 60 frames).

Movie S3 (.mov format). TIRF live imaging of TCR microcluster dynamics in a naïve CD8 OT-I T cell stimulated on an SLB and treated with 15 μ M SMIFH2 at 10 s after initial microcluster formation (2 s per frame; 75 frames).

Movie S4 (.mov format). TIRF live imaging of TCR microcluster dynamics in a naïve CD8 OT-I T cell stimulated on an SLB and treated with 15 μ M SMIFH2 at 20 s after initial microcluster formation (2 s per frame; 75 frames).

Movie S5 (.mov format). TIRF live imaging of cSMAC dynamics in a naïve CD8 OT-I T cell stimulated on an SLB for 10 min and treated with 15 μ M SMIFH2 (2 s per frame; 160 frames).

Movie S6 (.mov format). TIRF live imaging of TCR microcluster and LifeAct-EGFP dynamics in a control CD8 OT-I T blast stimulated on an SLB (2 s per frame; 60 frames).

Movie S7 (.mov format). TIRF live imaging of TCR microcluster and LifeAct-EGFP dynamics in a 10 μ M SMIFH2-treated CD8 OT-I T blast stimulated on an SLB (2 s per frame; 60 frames).

Movie S8 (.mov format). 3D reconstruction of a confocal image stack of pZap70 and F-actin staining in a control naïve CD8 OT-I T cell stimulated on an SLB for 1.5 min.

Movie S9 (.mov format). 3D reconstruction of a confocal image stack of pZap70 and F-actin staining in a 10 μ M SMIFH2-treated naïve CD8 OT-I T cell stimulated on an SLB for 1.5 min.

Movie S10 (.mov format). 3D reconstruction of a confocal image stack of pLAT and F-actin staining in a control naïve CD8 OT-I T cell stimulated on an SLB for 1.5 min.

Movie S11 (.mov format). 3D reconstruction of a confocal image stack of pLAT and F-actin staining in a 10 μ M SMIFH2-treated naïve CD8 OT-I T cell stimulated on an SLB for 1.5 min.

Movie S12 (.mov format). TIRF live imaging of TCR microcluster and EGFP-mDia1 dynamics in a CD8 OT-I T blast stimulated on an SLB (2 s per frame; 60 frames).

Movie S13 (.mov format). TIRF live imaging of TCR microcluster and EGFP-mDia3 dynamics in a CD8 OT-I T blast stimulated on an SLB (2 s per frame; 60 frames).

Movie S14 (.mov format). TIRF live imaging of TCR microcluster dynamics in a control naïve CD8 OT-I T cell stimulated on an SLB (2 s per frame; 60 frames).

Movie S15 (.mov format). TIRF live imaging of TCR microcluster dynamics in an mDia1/3 cDKO naïve CD8 OT-I T cell stimulated on an SLB (2 s per frame; 60 frames).

Movie S16 (.mov format). TIRF live imaging of TCR microcluster dynamics in a control OT-I thymocyte stimulated on an SLB (0.5 s per frame; 240 frames).

Movie S17 (.mov format). TIRF live imaging of TCR microcluster dynamics in an mDia1/3 cDKO (lck-cre) OT-I thymocyte stimulated on an SLB (0.5 s per frame; 240 frames).

Supplementary Materials and Methods

Antibodies and reagents

The following antibodies were used for FACS analysis: Fluorescein isothiocyanate (FITC)-conjugated antibodies to mouse CD4 (100510; RM4-5), TCR β (109206; H57-597), Gr-1 (108406; RB6-8C5) and CD49b (108906; DX5), phycoerythrin (PE)-conjugated antibody to mouse CD8a (100708; 53-6.7), Peridinin-chlorophyll-protein-complex with cyanine dye 5.5 (PerCP-Cy5.5)-conjugated antibodies to mouse CD45.1 (110727; A20), CD4 (100540; RM4-5) and CD44 (103032; IM7), and allophycocyanin (APC)-conjugated antibodies to mouse CD45.2 (109814; 104), CD8a (100712; 53-6.7), CD90.2 (105312; 30-H12) and mouse IgG1 (406609; RM01-1) were all from Biolegend. FITC-conjugated antibodies to mouse CD3 ϵ (553662; 145-2C11), CD8a (553031; 53-6.7), CD11b (553310; M1/70) and mouse IgG1 (553443; A85-1), and Alexa488-conjugated CD45R (557669; RA3-632) and APC-conjugated antibody to mouse IgG1 (560089; A85-1) were all from BD Pharmingen. FITC-conjugated antibody to mouse CD4 (11-0042-81A) and PE-conjugated antibody to mouse CD3 ϵ (12-0031-81; 145-2C11) were from eBioscience.

The following antibodies were used for western blotting: anti-pZap70 [Y319] (2719), anti-Zap70 (3165), anti-pLAT [Y191] (3584), anti-LAT (9166) and anti-SLP76 (4985) from Cell Signaling Technology, anti-pSLP76 [Y128] (558367) from BD Pharmingen, anti-mDia1 (610849) from BD transduction, anti-mDia3 (HPA005647) from Sigma-Aldrich, anti-GAPDH (AM4300) from Ambion, HRP-conjugated anti-mouse IgG (NA931V) and HRP-conjugated anti-rabbit IgG (NA934V) from GE Healthcare.

The following antibodies were used for immunocytochemistry: anti-mDia1 (610849) from BD transduction, anti-pZap70 [Y319] (2719), anti-pLAT [Y171] (3581), and Alexa555-conjugated anti-pZap70 [Y319] (custom order) from Cell Signaling Technology, Alexa 488-conjugated goat anti-mouse IgG (A11001) from Molecular Probes, and Cy2-conjugated donkey anti-mouse IgG (715-225-151), Cy3-conjugated goat anti-mouse IgG (115-166-003), Cy2-conjugated goat anti-rabbit IgG (111-225-003) and Cy3-conjugated donkey anti-rabbit IgG (711-165-152) from Jackson ImmunoResearch.

The following reagents were used for immunocytochemistry: Alexa 488-conjugated Phalloidin (A12379), Alexa 546-conjugated Phalloidin (A22283), Alexa 633-conjugated Phalloidin (A22284) and Hoechst 33342 (H3570) from Molecular Probes.

For preparation of the TCR-stimulatory lipid bilayer, dodecahistidine-tagged extracellular domain of ICAM1 (his-ICAM) was purified from the supernatants of High Five cells transfected with a baculovirus expression system using nickel-affinity resin followed by purification on MonoQ and then Superdex FPLC as previously described (23). Biotinylated H-2K^b loaded with SIINFEKL peptide (from US National Institutes of Health, Tetramer Facility) was used in monomeric form.

Western blotting

Cells were lysed in Laemmli buffer containing β -mercaptoethanol (21438-82, Nacalai). After sonication and denaturation at 96°C for 5 min, lysates were subjected to SDS-PAGE and the separated proteins then transferred to 0.45- μ m PVDF membranes (IPVH304FO, Millipore). The membranes were then blocked in 0.8% membrane blocking agent (RPN2125V, GE Healthcare), probed with the indicated primary antibody, washed and then incubated with HRP-conjugated secondary antibody. Immunoreactivity was detected using ECL prime Western Blotting Detection Reagent (RPN2232, GE Healthcare), and the chemiluminescence signal imaged using a ChemiDoc XRS imaging system (Biorad). Images were processed using Adobe Photoshop CS5 software (Adobe Inc.) and densitometry analysis was performed using ImageJ software (NIH).

Lipid bilayers

Lipid bilayers were prepared as previously described (23). Phospholipid mixtures consisting of 96.5% 1-plamitoyl-2-oleyl-sn-glycerol-3-phosphocholine (POPC), 2% 1, 2-dioleoyl-sn-glycero-3-[(N-(5-amino-1-carboxypentyl)iminodiacetic acid)succinyl]-nickel-nitrilotriacetic acid (Ni^{2+} -NTA-DGS), 1% 1, 2-dioleoyl-sn-glycero-3-phosphoethanolamine-N-cap biotinyl sodium (biotinyl-Cap-PE) and 0.5% polyethylene glycol 5,000-PE (1, 2-dioleoyl-sn-glycero-3-phosphoethanolamine-N-[methoxy(polyethylene glycol)-5000]), all purchased from Avanti Polar Lipids, were mixed in a round-bottom flask and dried. The next day, liposomes were prepared from rehydrated lipid cakes by extrusion through filters (pore size, 100 nm) with a Mini-Extruder set (Avanti Polar Lipids, 610000). For the setup of lipid bilayers, dilutions of liposomes were applied to a rigorously cleaned Lab Tek II chambered cover-glass (155409, Nalge Nunc). Excess liposomes were rinsed away, and bilayers were then blocked in 1% BSA/PBS. Streptavidin in 1% BSA/PBS was loaded onto the cover-glass and then the excess streptavidin was washed away. Biotinylated pMHC and his-ICAM were then loaded onto bilayers at a concentration of 25 ng/ml and 250 ng/ml, respectively. After protein loading, bilayers were rinsed and pre-warmed to 37°C before application of cells. Unless indicated otherwise, ‘stimulatory lipid bilayer (SLB)’ refers to a bilayer loaded with his-ICAM and pMHC under conditions that generate protein presentation similar to those generated by BMDCs pulsed with 100 ng/ml SIINFEKL peptide.

Quantitative reverse transcription–polymerase chain reaction (qRT-PCR)

mRNA was purified from naïve CD8 T cells using Reliaprep (Promega), and reverse-transcribed to cDNA using PrimeScript RT Master Mix (TaKaRa). cDNA, primers, and SYBR Premix ExTaq (Tli RNaseH Plus, TaKaRa) were mixed in 96-well PCR plates, and quantitative PCR was performed using a CFX96 Real-Time System (Bio-Rad). qRT-PCR data were analyzed using the $\Delta\Delta\text{CT}$ method. Primers used were as follows:

mDia1 F: 5'-CATCAATGCTCTCATCACTCC-3'

mDia1 R: 5'-CACCAAAGTCATCCATCTCC-3'

mDia2 F: 5'-ACCACACTCCTCCATTTCC-3'

mDia2 R: 5'-ACAAACTTGTCATGCAAGTCC-3'

mDia3 F: 5'- TCCTCCTCCTCCACCATTAC-3'

mDia3 R: 5'- CTTTAGGCTCAATCTTGGACC-3'

gapdh F: 5'-ATGACATCAAGAAGGTGGTG-3'

gapdh R: 5'-CATACCAGGAAATGAGCTTG-3'

ELISA

An IL2 ELISA kit (Biolegend, 431004) was used to measure levels of mouse IL2 in cell culture supernatants according to the manufacturer’s protocol.

Proliferation assay

Naïve CD8 T cells were plated in 96-well plates at 10^5 cells/well. Plate-bound anti-CD3 (1, 2, 4, 10 µg/ml) and soluble anti-CD28 (2 µg/ml) antibodies were used for TCR stimulation. Cell proliferation rate was assayed using a nonradioactive cell proliferation assay kit (Promega, G358A). Briefly, assays were performed by adding 20 µl of CellTiter 96 Aqueous One Solution Reagent

(MTS:[3-(4,5-dimethylthiazol-2-yl)-5-(3-carboxymethoxyphenyl)-2-(4-sulfophenyl)-2H-tetrazolium]) in 100 µl medium directly to each well, and the cells then cultured for a further 4 h at 37°C under 5% CO₂. The MTS compound is bio-reduced by cells into a colored formazan product that is soluble in culture medium and this was quantified by measuring the absorbance at 490 nm using a 96-well plate reader (Molecular Devices).

FACS analysis

For surface staining, single-cell suspensions from mouse thymus, spleen or peripheral blood were incubated with anti-CD16/CD32 antibody (553142, BD Pharmingen) for 10 min, stained with indicated mAbs for 30 min on ice, washed and then resuspended in FACS buffer (PBS containing 0.1% bovine serum albumin and 0.1% sodium azide). For intracellular staining of mDia1, cells were fixed and permeabilized using BD Cytofix/Cytoperm solution (554722, BD Biosciences), washed with BD Perm/Wash buffer (554723, BD Biosciences) and then labeled with mDia1 antibody for 1 h at room temperature or 4°C overnight. Quantitative flow cytometry data were acquired on a FACS Calibur (BD Biosciences) or LSR Fortessa (BD Biosciences) system and analyzed using FlowJo software (Tree Star Inc.).

Histology

After subjecting mice to deep anesthesia, the thymus was rapidly removed and fixed in 0.1 M sodium phosphate, pH 7.4, containing 4% paraformaldehyde. The thymus was then embedded in paraffin and cut into sections of 5-µm thickness. Hematoxylin and eosin (H&E) staining was performed using a standard protocol. Bright field images were acquired using an upright BX-50 microscope (Olympus) equipped with a color CCD camera (Optronics). Images were assembled with Stereo Investigator software (MBF Bioscience) and processed using Adobe Photoshop CS5 software (Adobe Inc.).

Bone marrow transplantation

For the transplantation of CD45.2 WT or mDia1/3 DKO donor bone marrow cells to CD45.1 recipients, CD45.1 congenic recipients were lethally irradiated at 9.5 Gy for 11 min before receiving 1×10^7 WT or mDia1/3 DKO bone marrow (BM) cells by intravenous injection. In the reverse setting, WT or mDia1/3 DKO mice were lethally irradiated before receiving CD45.1 congenic BM cells. BM chimeras were analyzed at 8 weeks after BM transplantation.

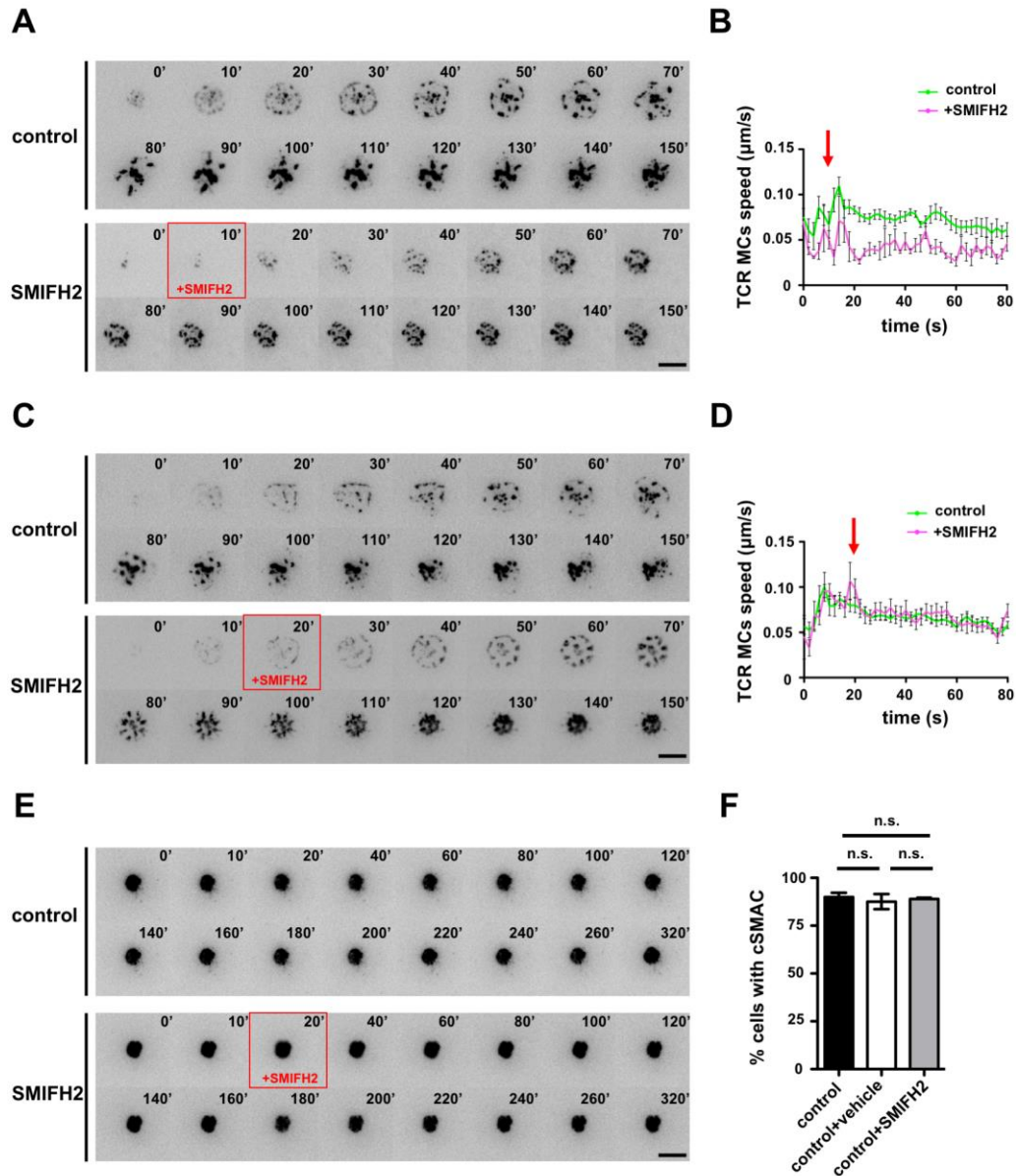


Fig. S1. Effects of formin inhibition after initial TCR microcluster formation in naïve CD8 OT-I T cells stimulated on SLBs. (A) TIRF images of TCR β -stained naïve CD8 OT-I T cells stimulated on a SLB. The indicated time is relative to the time of initial contact and TCR microcluster formation. SMIFH2 (15 μM) was added at 10 s after the initial contact. Scale bar, 5 μm . (B) Quantification of TCR microcluster average speed during the first 80 s as imaged in A. The graph shows average speed plotted against time. $n = 9$ for control cells and $n = 4$ for SMIFH2-treated cells. Red arrow indicates the addition of SMIFH2. Error bars represent SEM. (C) TIRF images of TCR β -stained naïve CD8 OT-I T cells stimulated on a SLB. The indicated time is relative to the time of initial contact and TCR microcluster formation. SMIFH2 (15 μM) was added at 20 s after the initial contact. Scale bar, 5 μm . (D) Quantification of TCR microcluster average speed during the first 80 s as imaged in C. The graph shows average speed plotted against time. $n = 13$ for control cells and $n = 5$ for SMIFH2-treated cells. Red arrow indicates the addition of SMIFH2. Error bars represented SEM. (E) TIRF images of the cSMAC in naïve CD8 OT-I T cells after stimulation on a SLB for 10 min. SMIFH2 (15 μM) was added 20 s after the commencement of time-lapse imaging. Scale bar, 5 μm . (F) Quantification of cSMAC formation in naïve CD8 OT-I T cells stimulated on a SLB for 10 min (control), or naïve CD8 OT-I T cells stimulated on a SLB for 10 min and then cultured for 5 min in the absence (control+vehicle) or presence (control+SMIFH2) of 15 μM SMIFH2 before fixation. Data are from three experimental replicates. n.s., not significant (one-way ANOVA with post hoc test).

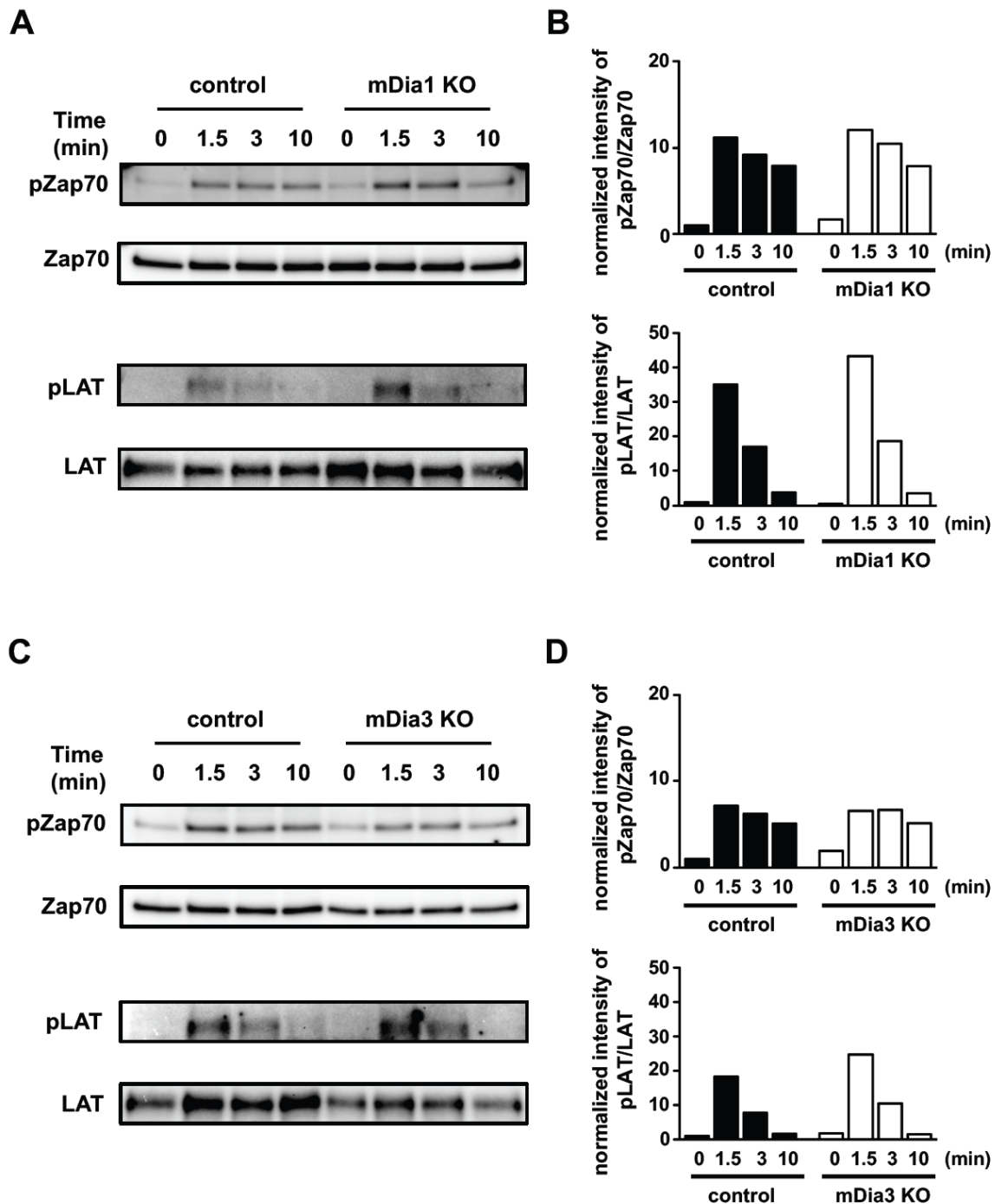


Fig. S2. TCR signaling in naïve CD8 T cells from mDia1 KO or mDia3 KO mice. (A) Western blotting analysis of total protein and pZap70 [Y319] and pLAT [Y191] in lysates of naïve CD8 T cell from control WT and mDia1 KO mice unstimulated (0) or stimulated for 1.5, 3 or 10 min with anti-CD3 (10 μ g/ml) and anti-CD28 (2 μ g/ml) antibodies. Data are representative of three independent experiments. (B) Densitometric quantification of the western blotting data in A. The value for the phosphorylated form relative to the total protein was normalized by the value obtained for unstimulated control cells. (C) Western blotting analysis of total protein and pZap70 [Y319] and pLAT [Y191] in lysates of naïve CD8 T cells from control WT and mDia3 KO mice unstimulated (0) or stimulated for 1.5, 3 or 10 min with anti-CD3 (10 μ g/ml) and anti-CD28 (2 μ g/ml) antibodies. Data are representative of three independent experiments. (D) Densitometric quantification of the western blotting data in C. The value for the phosphorylated form relative to the total protein was normalized by the value of obtained for unstimulated control cells.

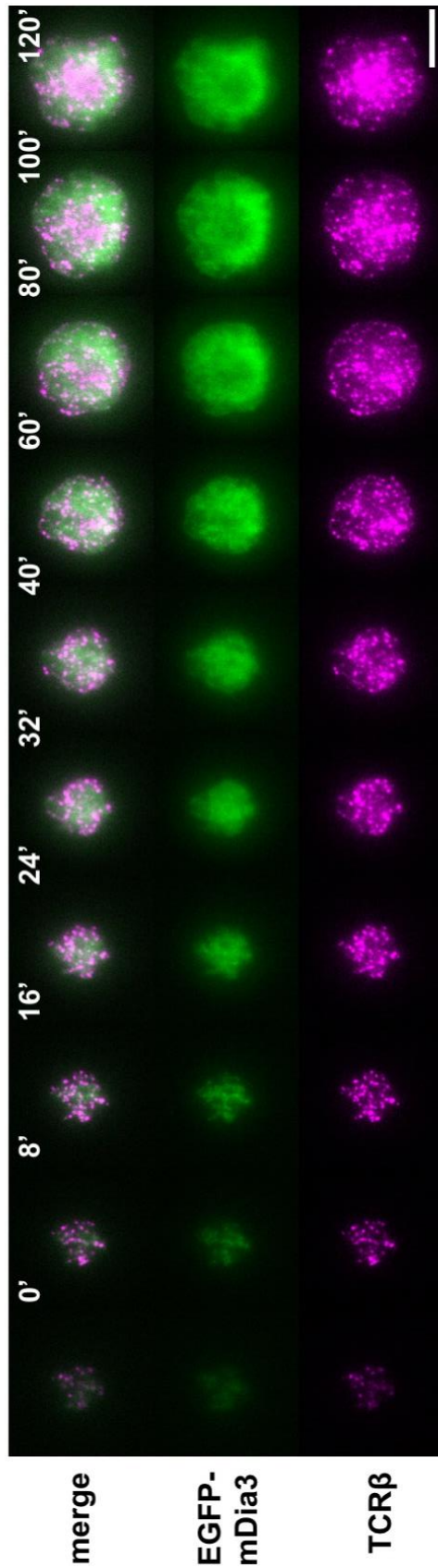


Fig. S3. Dynamic localization of EGFP-mDia3 in the IS. Representative TIRF images of TCR microclusters together with EGFP-mDia3 in CD8 OT-I T blasts stimulated on a SLB. Time is relative to the time of initial cell-SLB contact. Scale bar, 5 μ m.

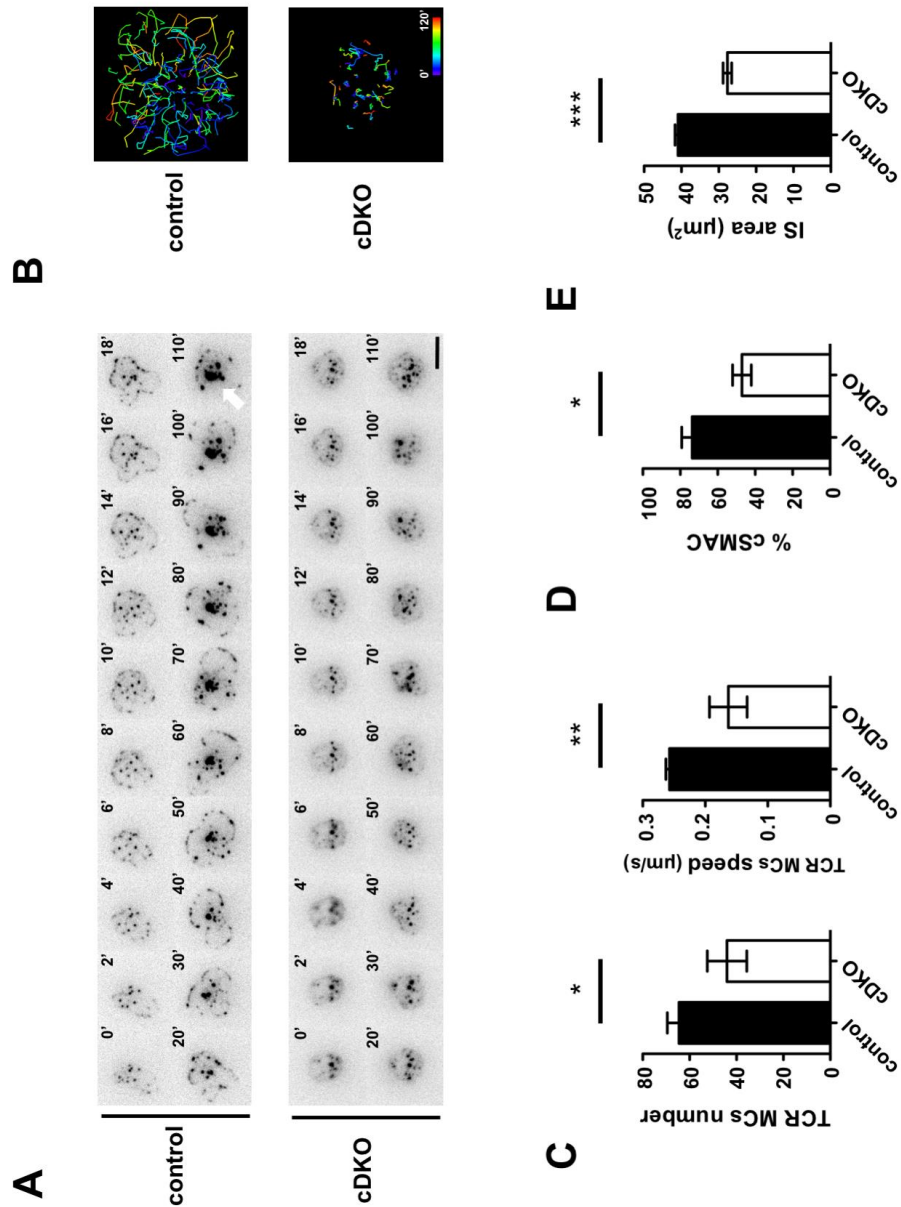


Fig. S4. IS spreading and TCR microcluster centralization are impaired in mDia1/3 cDKO naïve CD8 OT-I T cells. (A) Representative TIRF images of TCR microclusters in naïve CD8 OT-I T cells of control OT-I mice and tamoxifen-induced mDia1/3 cDKO OT-I mice stimulated on a SLB. The white arrow indicates the cSMAC in the control cell. Time is relative to the onset of IS spreading at 20 s. Scale bar, 5 µm. (B) Track plot of microcluster trajectories in A. Plots show the paths taken by individual microclusters over time (trajectory pseudocolor represents time as indicated in the key). (C) Quantification of TCR microcluster number and speed from imaging data shown in A. n = 12 for control cells and n = 9 for mDia1/3 cDKO cells. Data are shown as means ± SEM. n.s., not significant; *P < 0.05, **P < 0.01 (Student t-test). (D) Quantification of cSMAC formation in control and mDia1/3 cDKO naïve CD8 OT-I T cells fixed 10 min after stimulation on the SLB. Data are from four independent experiments. *P < 0.05 (Student t-test). (E) Quantification of IS area in control and mDia1/3 cDKO naïve CD8 OT-I T cells fixed 3 min after stimulation on the SLB. Results are from 106 control cells and 80 mDia1/3 cDKO cells. Data represent means ± SEM. *P < 0.05, ***P < 0.001 (Student t-test).

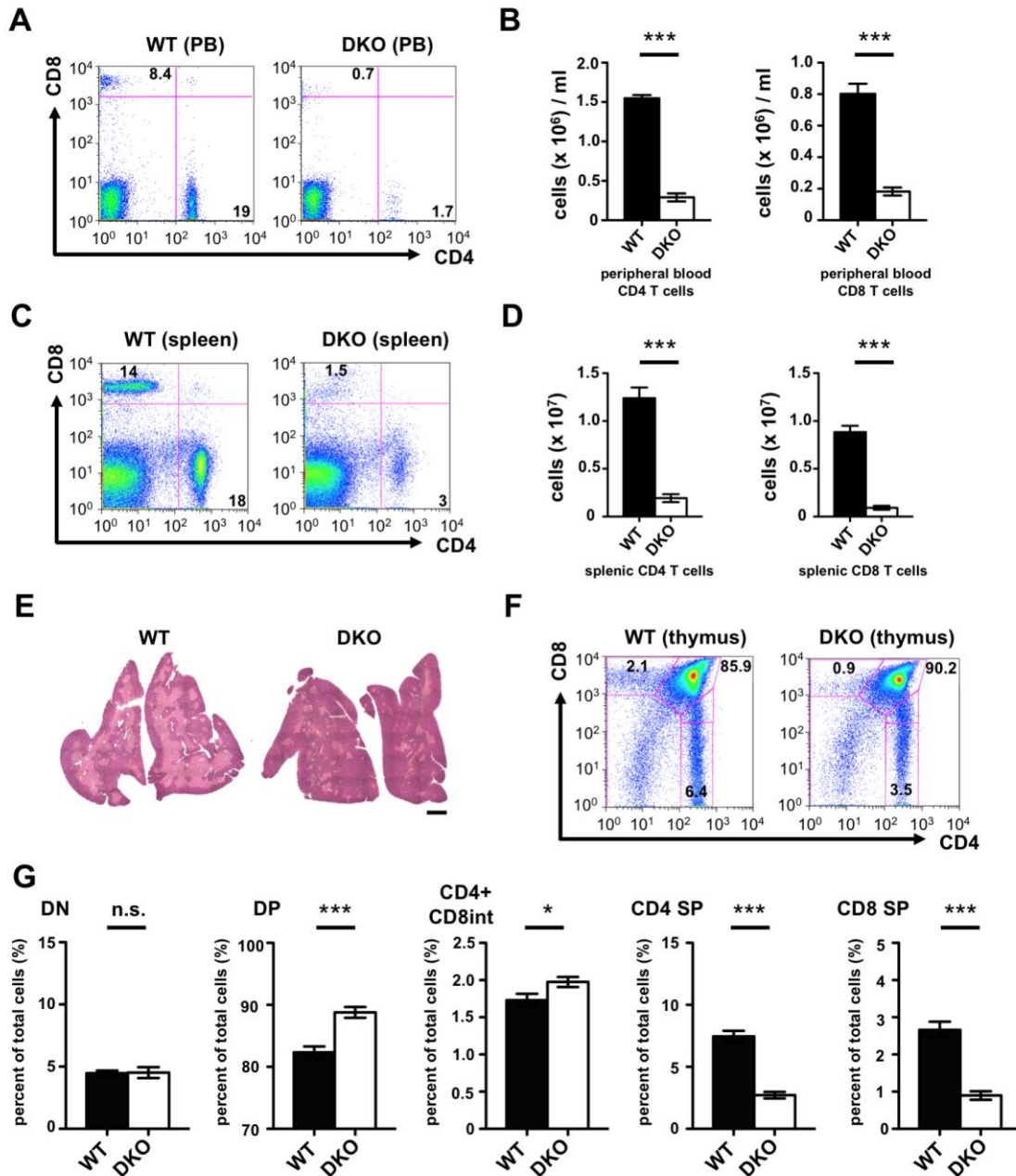


Fig. S5. T cell lymphopenia results from impaired positive selection in mDia1/3 DKO mice. (A) FACS analysis of surface CD4 and CD8 expression in WT and mDia1/3 DKO peripheral blood (PB) mononuclear cells from 8 to 10-week old mice. Numbers in the outlined regions indicate the cell percentage for each subpopulation. (B) Numbers of CD4 or CD8 T cells in peripheral blood from WT and mDia1/3 DKO mice. $n=3$. Data are shown as mean \pm SEM. *** $P < 0.001$ (Student t-test). (C) FACS analysis for surface CD4 and CD8 expression in WT and mDia1/3 DKO spleen from 8 to 10-week old mice. Numbers in the outlined regions indicate the cell percentage for each subpopulation. (D) Numbers of CD4 or CD8 T cells in spleen from WT and mDia1/3 DKO mice. $n=8$. Data are shown as mean \pm SEM. *** $P < 0.001$ (Student t-test). (E) Hematoxylin and eosin (H&E) staining of thymus sections from WT and mDia1/3 DKO mice. The cortex and medulla are indicated by dark and pale staining, respectively. Data are representative of four mice per group. Scale bar, 500 μm . (F) FACS analysis of surface CD4 and CD8 expression on thymocytes from 8 to 10-week old WT and mDia1/3 DKO mice. Numbers in the outlined regions indicate the percentage of cells for each thymocyte subpopulation. (G) Quantification of DN, DP, CD4+CD8int DP, CD4 SP and CD8 SP thymocyte subpopulations (21 mice per group). Data are shown as mean \pm SEM. n.s., not significant; * $P < 0.05$, *** $P < 0.001$ (Student t-test).

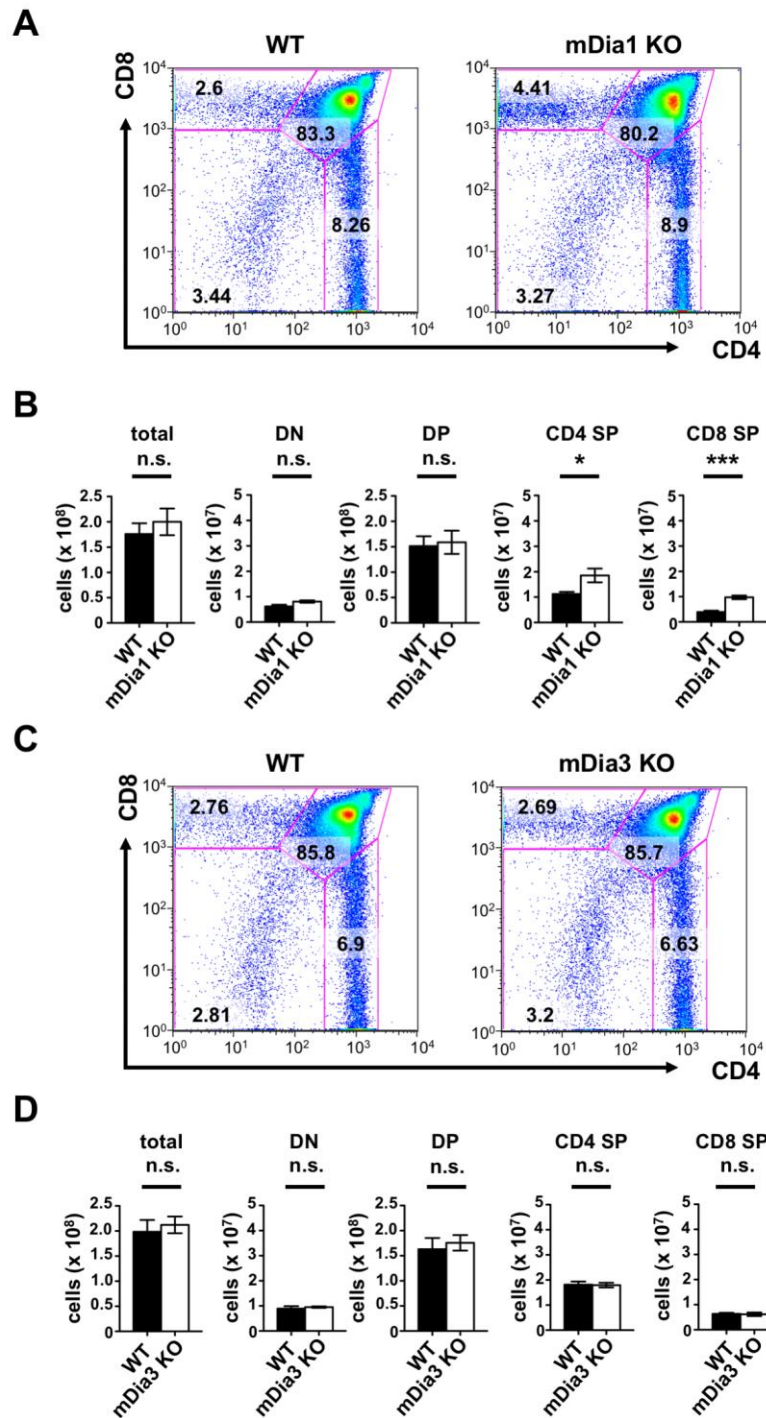


Fig. S6. T cell development in mDia1 KO mice and mDia3 KO mice. (A) FACS analysis for surface CD4 and CD8 expression on thymocytes from 8 to 10-week old WT and mDia1 KO mice. Numbers in the outlined regions indicate the percentage of cells in each thymocyte subpopulation. (B) Quantification of total, DN, DP, CD4 SP or CD8 SP subpopulations in the thymus of WT and mDia1 KO mice. Results from three independent experiments using five WT mice and three mDia1 KO mice are shown. Data are shown as mean \pm SEM. n.s., not significant, * $P < 0.05$, *** $P < 0.001$ (Student t-test). (C) FACS analysis of surface CD4 and CD8 expression on thymocytes from 8 to 10-week old WT and mDia3 KO mice. Numbers in the outlined regions indicate the percentage of cells in each thymocyte subpopulation. (D) Quantification of total, DN, DP, CD4 SP or CD8 SP subpopulations in the thymus of WT and mDia3 KO mice. Results from two independent experiments using eight mice per group are shown. Data are shown as mean \pm SEM. n.s., not significant (Student t-test).

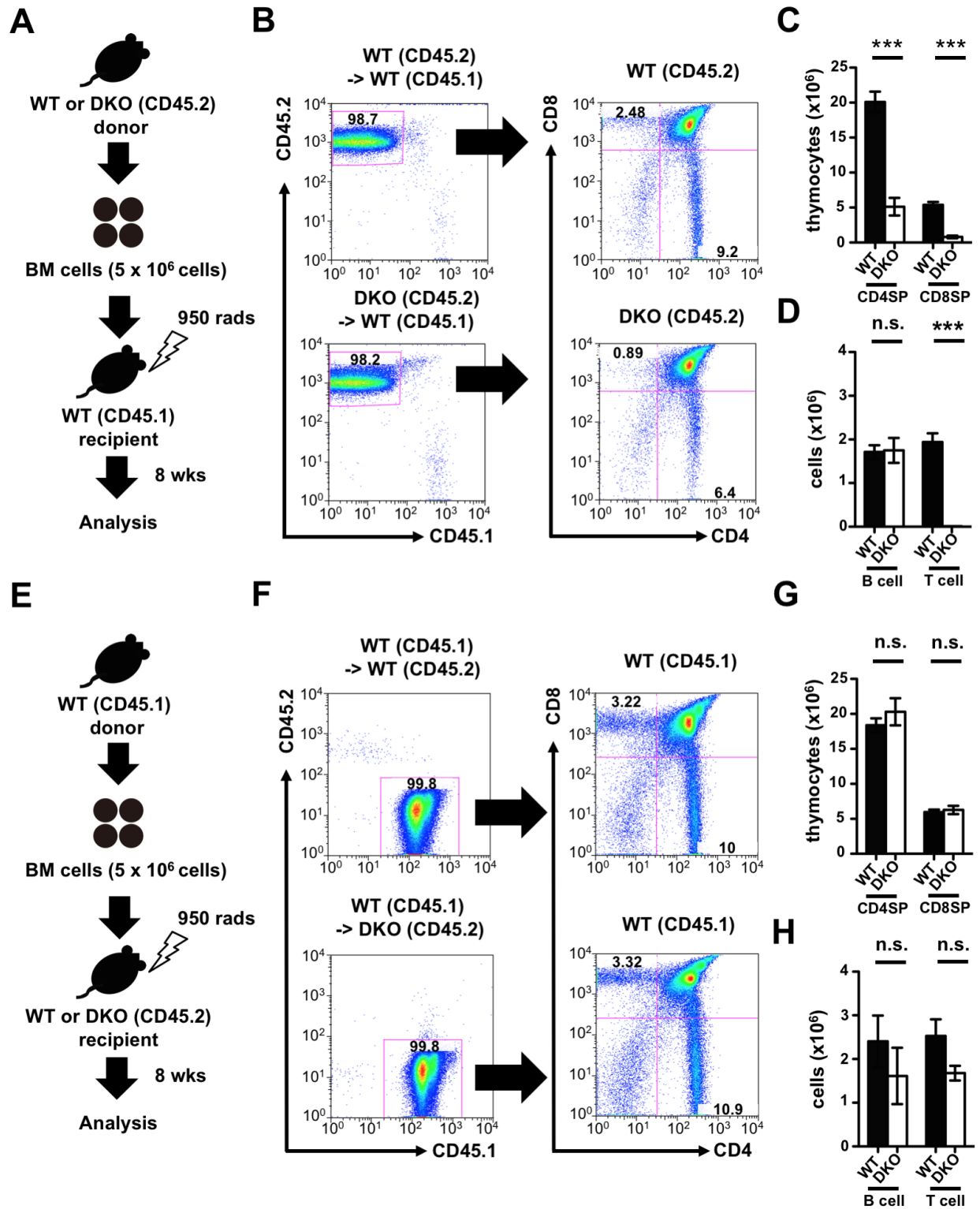


Fig. S7. Impaired T cell development phenotypes in mDia1/3 DKO are cell intrinsic. (A) Scheme of experimental design for bone marrow transplantation of WT (CD45.2) or mDia1/3 DKO (CD45.2) donor to WT (CD45.1) recipient. (B) FACS analysis of thymocytes from bone marrow chimeras 8 weeks after transfer of bone marrow cells from WT (CD45.2) mice or mDia1/3 DKO (CD45.2) mice into lethally irradiated WT (CD45.1) recipient mice. Surface expression of CD4 and CD8 (right) were assessed after gating on CD45.2 (left). Numbers in the outlined regions indicate the percentage of cells in each thymocyte subpopulation. Data are representative of three independent experiments with 8 mice for the WT (CD45.2) → WT (CD45.1) group and 5 mice for the mDia1/3 DKO (CD45.2) → WT (CD45.1) group. (C) Quantification of CD4 and CD8 surface expression on

thymocytes from three independent experiments with eight mice for the WT (CD45.2) -> WT (CD45.1) group and five mice for the mDia1/3 DKO (CD45.2) -> WT (CD45.1) group. Data represent mean \pm SEM. ***P < 0.001 (Student t-test). **(D)** Quantification of B cell and T cell numbers among splenocytes from three independent experiments using 8 mice for the WT (CD45.2) -> WT (CD45.1) group and five mice for the mDia1/3 DKO (CD45.2) -> WT (CD45.1) group. Data represent mean \pm SEM. n.s., not significant; ***P < 0.001 (Student t-test). **(E)** Scheme of experimental design for bone marrow transplantation of WT (CD45.1) to WT (CD45.2) or mDia1/3 DKO (CD45.2) donor recipients. **(F)** FACS analysis of thymocytes from bone marrow chimeras 8 weeks after transfer of bone marrow cells from WT (CD45.1) mice into lethally irradiated WT (CD45.2) or mDia1/3 DKO (CD45.2) recipient mice. Surface expression of CD4 and CD8 (right) were assessed after gating on CD45.1 (left). Numbers in the outlined regions indicate the percentage of cells in each thymocyte subpopulation. Data are representative of three independent experiments using six mice for the WT (CD45.1) -> WT (CD45.2) group and four mice for the WT (CD45.1) -> mDia1/3 DKO (CD45.2) group. **(G)** Quantification of CD4 and CD8 surface expression on thymocytes from three independent experiments using six mice for the WT (CD45.1) -> WT (CD45.2) group and four mice for the WT (CD45.1) -> mDia1/3 DKO (CD45.2) group. Data represent mean \pm SEM. n.s., not significant (Student t-test). **(H)** Quantification of B cell and T cell numbers among splenocytes from three independent experiments using six mice for the WT (CD45.1) -> WT (CD45.2) group and four mice for the WT (CD45.1) -> mDia1/3 DKO (CD45.2) group. Data represent mean \pm SEM. n.s., not significant (Student t-test).

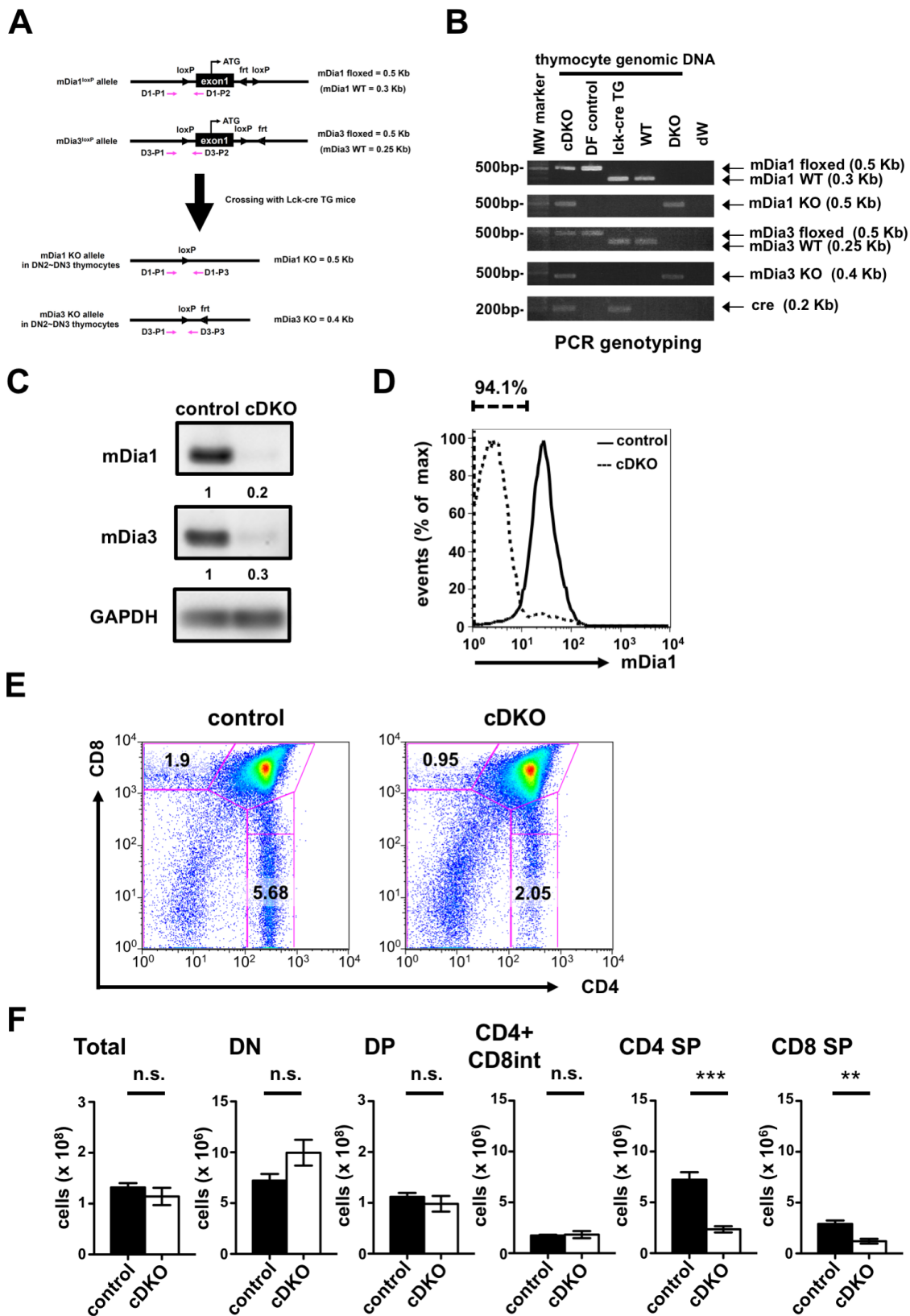


Fig. S8. Conditional deletion of mDia1 and mDia3 in the T cell lineage. (A) Lck-cre-mediated conditional deletion of mDia1 and mDia3. Magenta arrows indicate the PCR primers D1-P1 and D1-P2 for detection of mDia1 floxed and WT alleles, D1-P1 and D1-P3 for detection of the mDia1 KO allele, D3-P1 and D3-P2 for detection of mDia3 floxed and WT alleles, and D3-P1 and D3-P3 for detection of the mDia3 KO allele. (B) PCR genotyping confirmation of mDia1 and mDia3 double-deletion in thymocytes of mDia1/3 cDKO mice. (C) Confirmation of

mDia1 and mDia3 deficiency in mDia1/3 cDKO thymocytes by western blotting. Numbers below each lane indicate densitometric quantification of mDia1 and mDia3 levels relative to GAPDH and normalized to the value obtained for control mDia1/3 double-floxed cells. Data are representative of three independent experiments. **(D)** FACS analysis of mDia1 protein expression in control and mDia1/3 cDKO thymocytes. The dashed horizontal bar indicates the population of cDKO thymocytes negative for mDia1 expression (94.1% of total thymocytes). **(E)** CD4 and CD8 surface expression in control and mDia1/3 cDKO thymocytes from 10 to 14-week old mice. Numbers in the outlined regions indicate the percentage of CD4 and CD8 SP thymocytes. **(F)** Quantification of total, DN, DP, CD4+CD8int DP, CD4 SP or CD8 SP thymocyte subpopulations in mDia1/3 cDKO thymus. Results from eight control mice and seven mDia1/3 cDKO mice are shown, Bars represent mean \pm SEM. n.s., not significant; **P < 0.01, ***P < 0.001 (Student t-test).

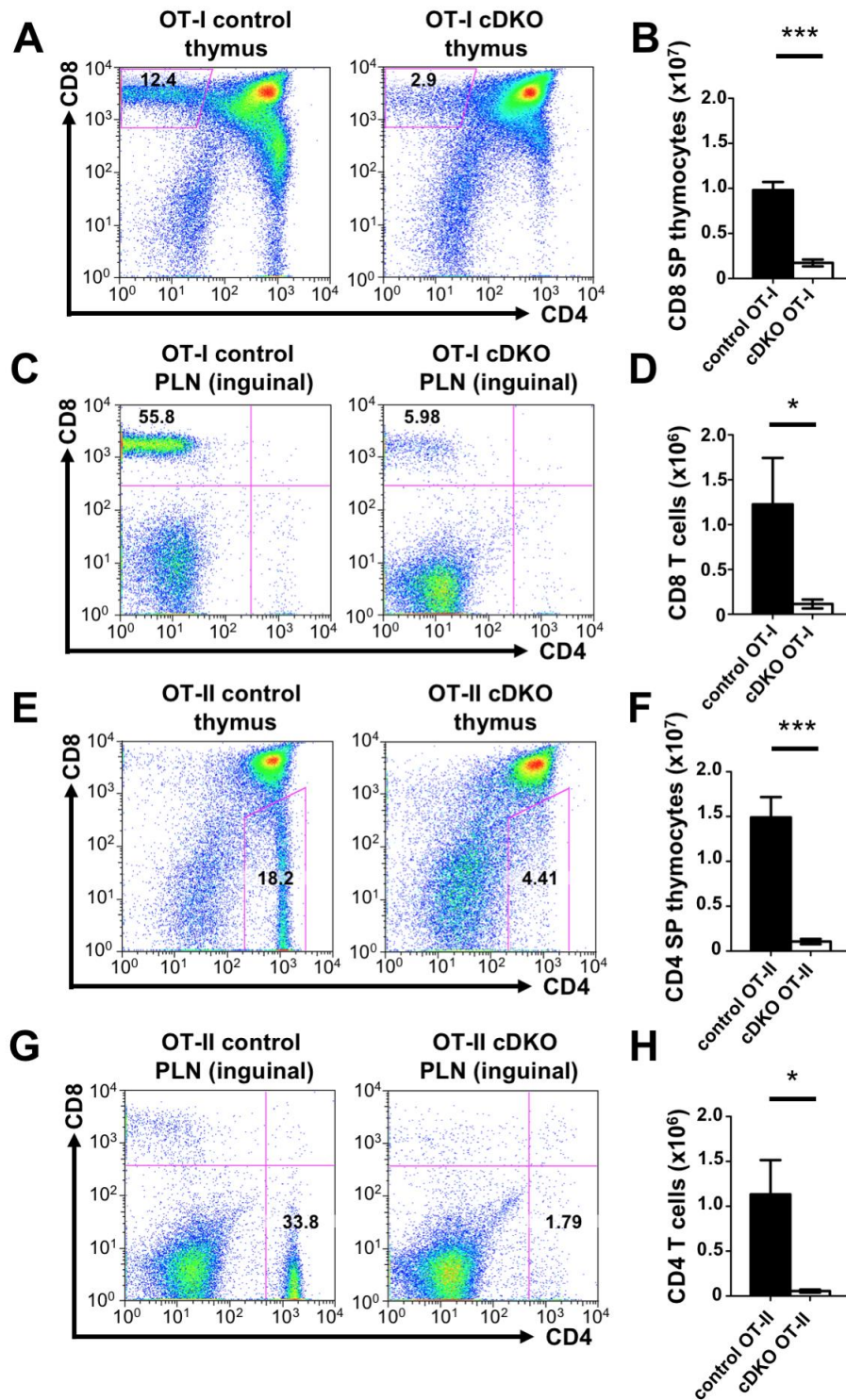


Fig. S9. mDia1/3 deficiency impaired thymocyte-positive selection in OT-I and OT-II transgenic mice. (A) FACS analysis of CD4 and CD8 surface expression in thymocytes from control mDia1/3 double-floxed mice or mDia1/3 cDKO (*lck-cre*) mice expressing a transgene encoding the MHC class I-restricted OT-I TCR. Numbers in the outlined regions indicate the percentage of CD8 SP thymocytes. Data are representative of two independent experiments using three mice for the control mDia1/3 double-floxed \times OT-I group and four mice for the cDKO \times OT-I group. (B) The total number of CD8 SP thymocytes from control OT-I and mDia1/3 cDKO (*lck-cre*) OT-I mice. Results from two independent experiments using three mice for the control mDia1/3 double floxed \times OT-I group and four mice for the cDKO \times OT-I group are shown, Bars represent mean \pm SEM. ***P < 0.001 (Student t-test). (C) FACS analysis of CD4 and CD8 surface expression in PLN cells (inguinal) from control mDia1/3

double-floxed mice or mDia1/3 cDKO (lck-cre) mice expressing the MHC class I-restricted OT-I TCR. Numbers in the outlined regions indicate the percentage of CD8 T cells. Data are representative of two independent experiments using three mice for the control \times OT-I group and four mice for the mDia1/3 cDKO \times OT-I group. **(D)** The total number of CD8 T cells in the PLN (inguinal) of control OT-I and mDia1/3 cDKO (lck-cre) OT-I mice. Results from two independent experiments using three mice for the control \times OT-I group and four mice for the mDia1/3 cDKO \times OT-I group are shown. Bars represent the mean \pm SEM. * $P < 0.05$ (Student t-test). **(E)** FACS analysis for CD4 and CD8 surface expression in thymocytes from control mDia1/3 double-floxed mice or mDia1/3 cDKO (lck-cre) mice expressing a transgene encoding the MHC class II-restricted OT-II TCR. Numbers in the outlined regions indicate the percentage of CD4 SP thymocytes. Data are representative of two independent experiments using four mice for the control mDia1/3 double-floxed \times OT-II group and seven mice for the cDKO \times OT-II group. **(F)** The total number of CD4 SP thymocytes from control OT-II and mDia1/3 cDKO OT-II mice. Results from two independent experiments using four mice for the control mDia1/3 double-floxed \times OT-II group and seven mice for the mDia1/3 cDKO (lck-cre) \times OT-II group are shown. Bars represent the mean \pm SEM. **** $P < 0.001$ (Student t-test). **(G)** FACS analysis of CD4 and CD8 surface expression in PLN cells (inguinal) from control mDia1/3 double-floxed mice or mDia1/3 cDKO (lck-cre) mice expressing the MHC class II-restricted OT-II TCR. Numbers in the outlined regions indicate the percentage of CD4 T cells. Data are from a single experiment using three mice for the control \times OT-II group and three mice for the mDia1/3 cDKO \times OT-II group. **(H)** The total number of CD4 T cells in the PLN (inguinal) of control OT-II and mDia1/3 cDKO (lck-cre) OT-II mice. Results are from a single experiment using three mice for the control mDia1/3 double-floxed \times OT-II group and three mice for the mDia1/3 cDKO (lck-cre) \times OT-II group are shown. Bars represent the mean \pm SEM. * $P < 0.05$ (Student t-test).

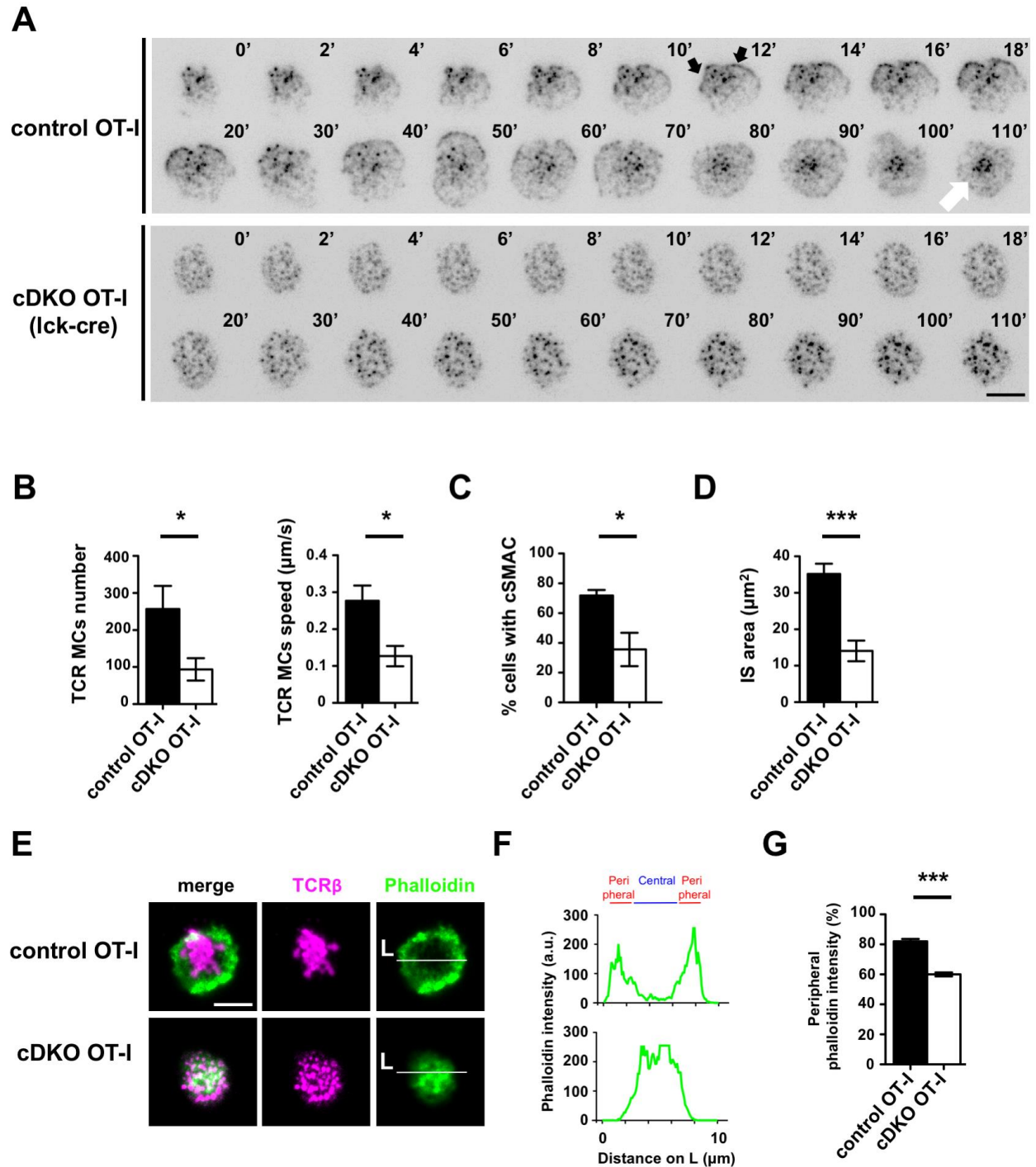


Fig. S10. Impaired TCR microcluster centralization and peripheral F-actin ring formation following loss of mDia1/3 in OT-I thymocytes. (A) Representative TIRF images of TCR microclusters in control OT-I or mDia1/3 cDKO (lck-cre) OT-I thymocytes stimulated on SLBs. Black arrows indicate the edge of spreading cell membrane and a white arrow indicates the cSMAC. Representative data from two independent experiments are shown. Scale bar, 5 μm . (B) Quantification of TCR microcluster number (left) and speed (right) in control mDia1/3 double-floxed OT-I ($n = 6$) and mDia1/3 cDKO (lck-cre) OT-I thymocytes ($n = 6$). Data are shown as mean \pm SEM. * $P < 0.05$ (Student t-test). (C) cSMAC formation in control mDia1/3 double-floxed OT-I or mDia1/3 cDKO (lck-cre) OT-I thymocytes stimulated on a SLB and then fixed after 10 min. Bars show the percentage of cells with cSMAC for each experimental group. Data were quantified from three independent experiments and are shown as the mean \pm SEM. * $P < 0.05$ (Student t-test). (D) Quantification of IS area in control mDia1/3 double-floxed OT-I and mDia1/3 cDKO (lck-cre) OT-I thymocytes fixed 3 min after stimulation on SLBs. Results are from 27 control cells and 19 mDia1/3 cDKO cells. Data represent means \pm SEM. *** $P < 0.001$ (Student t-test). (E) Representative TIRF images

of TCR microclusters and F-actin (phalloidin) in control mDia1/3 double floxed OT-I or mDia1/3 cDKO (lck-cre) OT-I thymocytes stimulated on a SLB and then fixed at 10 min. Scale bar, 5 μ m. **(F)** Linescan profile of the signal intensities of Phalloidin along the white line “L” shown in (E). “Central” is defined as the half radius area from cell center and “Peripheral” is defined as the remaining area. **(G)** Peripheral F-actin amounts (phalloidin fluorescence intensity) in control mDia1/3 double floxed OT-I (n=10) or mDia1/3 cDKO (lck-cre) OT-I thymocytes (n=10) stimulated on SLBs and then fixed at 10 min. Data are shown as mean \pm SEM. ***P<0.001 (Student t-test).